Synthesis and characterization of a novel organic corrosion inhibitor for mild steel in 1 M hydrochloric acid

Mohammed H. Othman Ahmed [a], Ahmed A. Al-Amiery [b,*], Yasmin K. Al-Majedy [b], Abdul Amir H. Kadhum [a], Abu Bakar Mohamad [a], Tayser Sumer Gaaz [c,*]

[a] Department of Chemical & Process Engineering, Faculty of Engineering & Built Environment, Universiti Kebangsaan, Malaysia
[b] Energy and Renewable Energies Technology Center, University of Technology, Baghdad 10001, Iraq
[c] Department of Machinery Equipment Engineering Techniques, Technical College Al-Musaib, Al-Furat Al Awsat Technical University, Al-Musaib, Babil 51009, Iraq

ARTICLE INFO

ABSTRACT

The synthesis and characterization of a novel organic corrosion inhibitor (4-(3-mercapto-5,6,7,8-tetrahy dro-[1,2,4]triazolo[4,3-b][1,2,4,5]tetrazin-6-yl)phenol), for mild steel in 1 M hydrochloric acid (HCl) has been successfully reported for the first time. The inhibitor evaluated as corrosion inhibitor for mild steel in 1 M of Hydrochloric acid solution using electrochemical impedance spectroscopy (EIS), and electro-chemical frequency modulation (EFM) measurement techniques. Changes in the impedance parameters suggested an adsorption of the inhibitor onto the mild steel surface, leading to the formation of protective films. The results show that the inhibition efficiencies increased with increasing the concentrations of the inhibitors and decreased with increasing temperature. The maximum inhibition efficiency up to 67% at the maximum concentration 0.5 mM. This shows that those inhibitors are effective in helping to reduce and slowing down the corrosion process that occurs to mild steel with a hydrochloric acid solution by providing an organic inhibitor for the mild steel that can be weakened by increasing the temperature. The adsorption process of the synthesized organic inhibitor depends on its electronic characteristics in addition to steric effects and the nature of metal surface, temperature degree and the varying degrees of surface-site activity. The synthesized inhibitor molecules were absorbed by metal surface and follow Langmuir isotherms.

Introduction

Mild steel, also known as low carbon steel, is a low cost and remarkable material in industrial technology because it is extensively used in chemical and allied industries for the handling of acid, alkali and salt solutions [1]. However, its tendency to corrode makes it unsuitable for exposure to acids. The use of inhibitors is one of the most practical methods for protection against corrosion in acidic media [2]. Corrosion inhibitors are chemical compounds that in small quantities can retard the degradation of metals in hostile environments [3]. Organic inhibitors have been widely used due to the ability of these compounds to prevent corrosion in various corrosive environments [4]. These compounds can adsorb onto the mild steel surface and block active sites, thus decreasing the corrosion rate [5]. In addition, a variety of organic compounds have been reported to be effective as corrosion inhibitors during acidization in industrial cleaning processes [6]. Organic additives prevent the adsorption of chloride ions and/or the formation of a more resistant oxide film on the metal surface [7]. The inhibition efficiency of these compounds depends mainly on the structure and nature of the adsorbed layer on the metal surface [8]. Organic compounds, mainly containing nitrogen, oxygen, sulfur and phosphorus atoms and having multiple bonds, are recognized as effective inhibitors for the corrosion of many metals and alloys [9]. O, N, S and P, they found to act as corrosion inhibitors due to their active centers for the process of adsorption on metal surfaces, higher basicity as well as electron density. The inhibition efficiency should follow the sequence O < N < S < P [10]. Adsorption depends mainly on certain physicochemical properties of the inhibitor group, such as electron density at the donor atom and orbital character and electronic structure of the molecule [11]. The adsorption of organic molecules at the metal/solution interface is of great interest in surface science and can markedly change the corrosion resistance of the metal [12]. It is generally accepted that the first step in the adsorption of an organic inhibitor on a metal surface usually

---

* Corresponding authors.
E-mail addresses: dr.ahmed1975@gmail.com (A.A. Al-Amiery), taysersumer@gmail.com (T.S. Gaaz).

involves replacement of one or more water molecules adsorbed at the metal surface [13]. The inhibitor may then combine with freshly generated Fe2+ ions on the steel surface, forming metal inhibitor complexes [14]. The organic inhibitors function through adsorption on the metal surface blocking the active sites by displacing water molecules and forming a compact barrier film to decrease the corrosion rate [15]. Acid solutions are widely used in industrial applications, such as acid pickling, industrial acid cleaning, acid descaling and oil well acidizing. As of result of the general aggressiveness of acid solutions, inhibitors are commonly used to reduce corrosive attack on metallic materials [16].

In continuation of previous work [17–20], we focus herein on the design our approach to increase the inhibitive properties based on conjugated system and electron density, so to the best of our knowledge novel corrosion organic inhibitor namely 4-(3-mercapto-5,6,7,8-tetrahydro-[1,2,4]triazolo[4,3-b][1,2,4,5] tetrazin-6-yl)phenol has been successfully synthesized and employed as a corrosion inhibitor for mild steel in 1 M hydrochloric acid. The inhibitory effect was investigated using various electrochemical measurement techniques such as Electrochemical Impedance Spectroscopy (EIS), and electrochemical frequency modulation (EFM).

Materials and methods

Chemistry

Synthesis of corrosion inhibitor (4-(3-mercapto-7,8-dihydro-[1,2,4]triazolo[4,3-b][1,2,4,5] tetrazin-6-yl)phenol). Mixture of 4-hydroxybenzaldehyde (1.22 g, 10 mmol) and 4-amino-5-hydrazinyl-4H-1,2,4-triazole-3-thiol (Purpald) (1.46 g. 10 mmol) with ferric ammonium sulfate (5.0 g, 10 mmol) in water (50 mL) was reacted under reflux condition. After 6 h, a solution of ferric ammonium sulfate (20 mmol, 10 g) in water (50 mL) was added to the mixture of reaction. The reaction continued for 4 h, the progress of the reaction was monitored by TLC, using ethyl acetate: n-hexane (1:1). The mixture of the reaction was cold; the precipitate was filtered, washed with water, dried and recrystallized by ethanol. IR: 3305.1 and 3278.8 cm^{-1} (NH), 3155 cm^{-1} (O—H), 3082.5 cm^{-1} (C—H; aromatic group), and 16132.9 cm^{-1} (C=N). ^1H NMR (δ 2.053 for Acetone as a solvent): δs, 2.935 NH; s, 3.298 NH; 5.1 OH; dd 6.990 and 7.004 for CH aromatic; dd 7.775 and 7.790 for CH aromatic; 9.837 for SH. 13C NMR (Acetone solvent has δ29.45 and 206.31): 116.45C—H for OH—C=C—H; 125.25 = C—C; (127.39, 129.24, 130.43, 132.79 Aromatic carbons), 146.41C=N, 159.89C—OH; 161.71C=N; 163.99N=C—SH.

To synthesize (4-(3-mercapto-5,6,7,8-tetrahydro[1,2,4]triazolo [4,3-b][1,2,4,5]tetrazin-6-yl) phenol) as a corrosion inhibitor, the reaction sequence outlined in Fig. 1 was followed, starting from commercially available 4-hydroxybenzaldehyde and (Purpald).

Electrochemical measurements

Mild steel specimens were obtained from Gamry Instruments Inc. and were used as working electrodes throughout this study, each with an active surface area of 4.5 cm^2. The composition (wt

%) of the mild steel was as follows: Fe, 99.21; C, 0.21; Si, 0.38; P, 0.09; S, 0.05; Mn, 0.05; and Al, 0.01. The specimens were cleaned according to ASTM standard procedure G1-03 [21]. Measurements were conducted in aerated, non-stirred 1.0 M HCl solutions containing different concentrations of the inhibitor. Electrochemical measurements were performed at the steady-state corrosion potential using a Gamry euro cell. The cell contained three electrodes, working, counter and reference electrodes, which were composed of mild steel, a graphite bar and a saturated calomel electrode (SCE), respectively. The measurements were performed using the Gamry Instrument Potentiostat/Galvanostat/ZRA (REF 600) model (Gamry, Warminster, PA, USA). DC105 and EIS300 software by Gamry were used to perform the corrosion potential, electrochemical impedance spectroscopy (EIS) and electrochemical frequency modulation (EFM) measurements. EIS measurements were performed using the AC signals of the 5 mV peak-to-peak amplitude at the corrosion potential in the frequency range of 100 kHz to 0.1 Hz. All impedance data were fit to appropriate equivalent circuits (ECs) using the Gamry Echem Analyst software. EFM measurements were carried out at 0.1 Hz base frequency with applied AC potential of 10 mV for 20 cycles. The electrochemical measurements began to be collected approximately 30 min after the working electrode was immersed in the solution to allow the steady state potential to stabilize. Each measurement was repeated five times, and only the average values were reported to verify reproducibility of the experiments.

Results and discussion

Synthesis

The synthesis was carried out by refluxing purpald with 4-hydroxybenzaldehyde in the presence of with ferric ammonium sulfate. The molecular weight of the synthesized corrosion inhibitor was 248 g/mol that was calculated based on the molecular formula ($C_9H_8N_6OS$) and supported via mass spectrometry. (4-(3-mercapto-5,6,7,8-tetrahydro-[1,2,4]triazolo[4,3-b][1,2,4,5] tetrazin-6-yl)phenol) can be dissolved in acetone, dichloromethane, dimethylformamide, dimethylsulfoxide, ethanol or methanol solutions. Fig. 2- SI, shows a proton-NMR spectrum for the corrosion inhibitor in which absorption bands at 3305.1 and 3278.8 cm^{-1} for amine NH and azomethane (C=N) and stretching at 16132.9 cm^{-1} can be seen. The bands at 3155 and 3082.5 cm^{-1} are from O—H and C—H aromatic respectively. The ^1H NMR spectrum exhibits two singlet signals at δ2.935 ppm an 3.298 ppm due to the N—H protons groups respectively, δ 5.100 (s, 1H, for OH), and δ6.990 (d, ^1H), 7.004 (s, ^1H), 7.775 (d, ^1H) and 7.790 (s, ^1H) for aromatic ring, also at δ9.837 (s, ^1H, for —SH) (Fig. 2- SI).

Fig. 3- SI, illustrates a ^{13}C NMR, spectrum for the corrosion inhibitor in which a signal appears at 163.99 ppm due to the N=C—SH group also 159.89 ppm and 146.41 ppm are from hydroxyl and azomethane groups respectively. Bands at 127.39, 129.24, 130.43 and 132.79 ppm are from carbon atoms in the aromatic ring.

Electrochemical results

Electrochemical impedance spectroscopy (EIS)

EIS is another method to test the effectiveness of corrosion inhibitors that is used to protect the surface of the mild steel in the acidic solution (1M HCl). Different corrosion system (e.g., charge transfer control, diffusion control or a mixture type) may show different features in the EIS spectra. Through analyzing the EIS data (Nyquist plot), the corrosion mechanism of the system can be identified. In practice, EIS data are often interpreted in terms of electrical equivalent circuits that can be used to describe the electrical
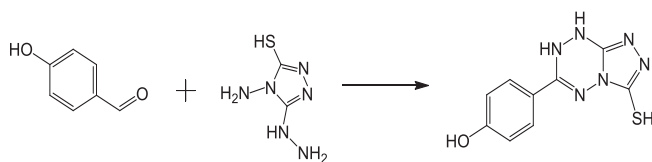

Fig. 1. Chemical synthesis of inhibitor.

features of the electrochemical interfaces [22]. The Nyquist plot contains a "depressed" semicircle with the center under the real axis, such behavior characteristic for solid electrodes and often referred to as frequency dispersion, which have been attributed to roughness and inhomogeneity of the surface [23]. Two ways are used in the literature to describe the EIS spectra for the inhomogeneous films on the metal surface or rough and porous electrodes. One is the finite transmission line model [24] and the other is the filmed equivalent circuit model [25], which is usually proposed to study the degradation of coated metals [26]. It has been suggested that the EIS spectra for the metal covered by organic inhibitor films are very similar to the failed coating metals [27]. The tests were carried out at 30 °C with the absence and the presence of different concentrations of the corrosion inhibitor ranging from 0.030 to 0.050 mM as shown in Fig. 2.
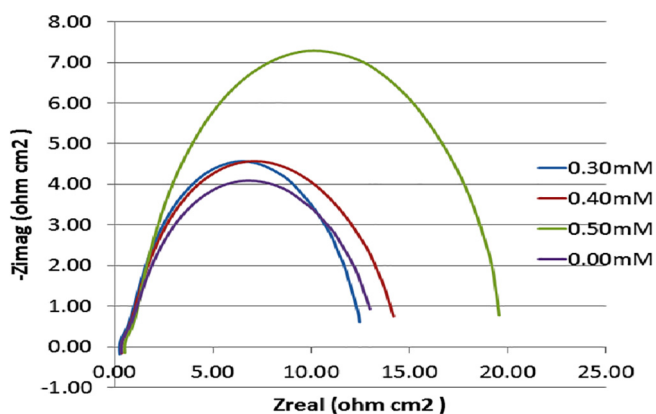

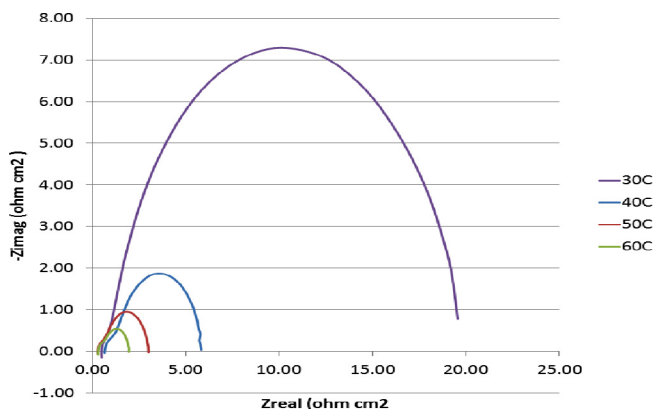**Fig. 2.** Nyquist plots for mild steel in 1.0 M HCl with various concentrations of the inhibitor at 30 °C.

Fig. 3. Nyquist plots for mild steel in 1.0 M HCl with 0.5 mM of the inhibitor at various temperatures ranging from 30 to 60 °C.

As shown in Fig. 3, the impedance response of mild steel is significantly altered after the addition of inhibitor to the corrosive solution. This result can be attributed to an increase in the substrate impedance with increased inhibitor concentration. The next experiments is using the same concentration of corrosion inhibitor that is 0.5 mM but at different temperatures which were 30, 40, 50 and 60 °C.

Based on Fig. 3, we can see that the graph of semi-circle at 60 °C is the smallest and at 30 °C was greatest. This shows that the diameter of the semi-circle is getting smaller with increasing temperature. These results suggest that the inhibition of corrosion is significantly reduced with increasing temperature. Increasing the temperature of the solution accelerates the corrosion process that occurs due to changes in the operating mechanism of corrosion [28]. From Fig. 3, the total impedance of mild steel in the presence of 0.5 mM decreases with increasing solution temperature. This behavior is due to desorption of adsorbed inhibitor molecules from the mild steel surface. The experimental data for the two Figs. are summarized in Tables 1 and 2. There is a considerable increase in the total impedance observed with the addition of corrosion inhibitor as shown in Tables 1 and 2. In the impedance spectrum of mild steel in the presence of response, the Nyquist plots have two loops: one loop in the high frequency region (HF) and another at an intermediate frequency (MF), with slight inductive behavior at low frequencies (LF). The HF and MF loops are attributed to the electrode and charge-transfer process, respectively. The inductive behavior observed in the LF region is attributed to relaxation of the adsorption of corrosion products or to the adsorption of inhibitor molecules on the mild steel surface in acidic solution in the absence and presence of inhibitor, respectively [29–30]. Similar behavior is observed for all temperatures examined. The corroding surface of the working electrode is expected to be inhomogeneous due to its roughness; therefore, the capacitance is presented through a constant phase element (CPE). The EIS results were analyzed using the equivalent circuit mentioned elsewhere [31], as shown in Fig. 4. The inhibition efficiencies (IE%) were calculated from the charge transfer resistance using the Eq. (1):

$$(IE\%) = (R_p^{\circ} - R_p / R_p^{\circ}) \times 100 \tag{1}$$

where R_p^o and R_p indicate the charge transfer resistances in the presence and absence of corrosion inhibitor, respectively.

By using the Gamry Analyst software, EIS experimental data can be obtained with CPE data matching. In Table 1, R_s is the solution resistance, CPE is the constant phase element, R_p, is the charge transfer resistance and C_{dl} is the double layer charge [32]. Table 1 shows the EIS data for 1.0 M HCl with different corrosion inhibitor concentrations at 30 °C, where the C_{dl} values decrease and the R_p values increase with the increasing of inhibitor concentrations. This is due to the gradual replacement of water molecules by the adsorption of the inhibitor molecules on the metal surface, and decreasing the extent of dissolution reaction. The high R_p values are generally associated with slower corroding system [33]. While the decrease in C_{dl} values resulted from the decrease of the local dielectric constant and/or from the increase of thickness of the electrical double layer [34]. The corrosion inhibitor molecules

Table 1
CPE data for mild steel in 1.0 M HCl with different corrosion inhibitor concentrations at 30 °C.

Concentration (mM)	R_s (ohm cm^2)	R_p (ohm cm^2)	CPE_{dl}		CPE_{dl}	IE
			Y_o (μSs^a cm^{-2})	a	(μF cm^{-2})	(%)
Blank	1.71	1.71	8983	0.65	152,400	0.00
0.30	3.02	3.02	7208	0.70	181,400	43.45
0.40	3.57	3.57	6473	0.69	156,600	52.07
0.50	4.21	4.21	4134	0.73	116,800	59.36

Table 2
CPE data for mild steel in 1.0 M HCl with 0.5 mM corrosion inhibitor at different temperatures.

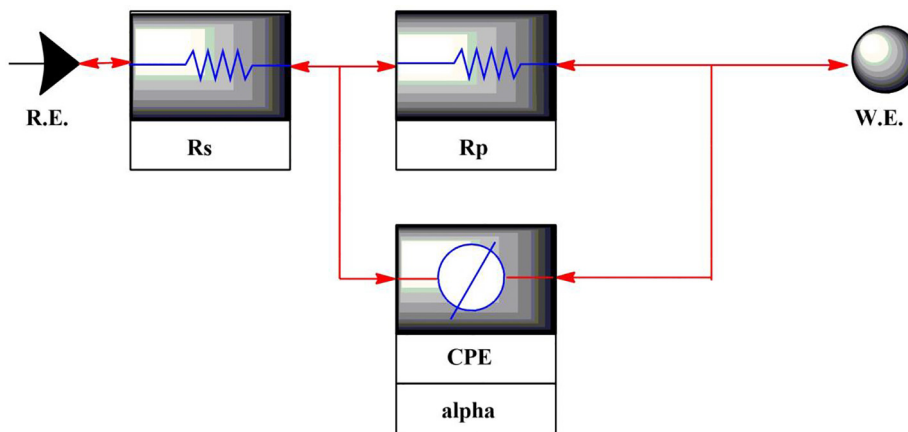| Temp. (°C)	Concentration (mM)	R_s (ohm cm^2)	R_p (ohm cm^2)	CPE_{dl}		CPE_{dl}	IE
				Y_o (μSs^a cm^{-2})	a	(μF cm^{-2})	(%)
30	Blank	1.71	1.71	8983	0.65	152,400	0.00
30	0.50	4.208	4.208	4134	0.73	116,800	59.36
40	Blank	2.77	2.77	21,880	0.58	2,531,000	0.00
40	0.5	3.96	3.96	11,320	0.61	1,238,000	30.05
50	Blank	1.60	1.60	5118	0.73	4,448,000	0.00
50	0.5	2.17	2.17	1145	0.62	4,035,000	26.27
60	Blank	1.51	1.52	5071	0.73	14,460,000	0.00
60	0.5	1.92	1.88	1155	0.63	11,120,000	19.15

Fig. 4. Equivalent model used to fit impedance data for mild steel in 1.0 M HCl in the absence and presence of the inhibitor.

absorbed on the surface of mild steel samples form a protective layer on the mild steel. Great resistance transfer charges commensurate with systems that corrode slowly. With the increase in the value of R_p, the efficiency of inhibition (IE) also increased.

Table 2 illustrates that the R_p and inhibition efficiency (IE) decreased when the temperature increased from 30 to 60 °C. This could be attributed to the fact that corrosion inhibitor molecules which are adsorbed on the surface of the mild steel will undergo condensation when the temperature increases [35]. Adsorption of organic compounds can be divided into two main types, physical adsorption and interaction 'chemisorption'. The presence of a metal having vacant low energy electron orbital of and of an inhibitor with molecules having relatively loosely bound electrons or heteroatoms with lone pair electrons. However, the compound reported is an organic base which can be protonated in an acid medium [36]. As shown in Tables 1 and 2, the R_p values increase with increasing concentration but decrease significantly with increasing solution temperature. Fig. 4 illustrates the circuit model employed in this work.

Electrochemical frequency modulation (EFM)

Electrochemical frequency modulation (EFM) is a new corrosion measurement technique for determining corrosion rate without preliminary knowledge of the Tafel constants [37]. The main advantage of this technique is that corrosion rate, Tafel parameters and causality factors are measured in a single data set [38]. While using EFM, a potential perturbation signal composed of two sine waves is applied to any corroding specimen to obtain a current response. EFM has been used for different combinations of metals and electrolytes to accurately measure corrosion parameters. This technique is similar to the harmonic method which employs a lower-amplitude (20 mV) sinusoidal perturbation signal but, unlike the harmonic method, is composed of two sine waves

instead of one. EFM has many advantages over the harmonic method, including data validations, a larger current response and an insensitivity to harmonics in the perturbation signal.

The inhibition efficiencies of the corrosion inhibitors (IE) were calculated using the Eq. (2).

$$IE(\%) = (i_{corr}^{\circ} - i_{corr}/i_{corr}^{\circ}) \times 100 \tag{2}$$

where i_{corr}° and i_{corr} are the corrosion current density without and with corrosion inhibitor.

Table 3 shows the electrochemical parameters of EFM for mild steel in 1.0 M HCl at 30 °C with different concentrations of the corrosion inhibitor. i_{corr} decreases by increasing the inhibitor concentration. The corrosion rate decreased from 174.81mpy to 62.75 mpy which demonstrates the effectiveness of the corrosion inhibitor. The standard values for CF-2 and CF-3 are 2.0 and 3.0, respectively. If causality factors differ from 2 to 3, one may conclude that the measurement is affected by noise. If the value of the causality factor approximates the standards, a correlation exists between the perturbation and response signals; therefore, the data are accepted. If CF-2 and CF-3 are in the range of 0–2 and 0–3, the EFM data are valid. Any deviation in the causality factor from the theoretical value may be due to perturbation amplitude that is too small, in insufficient resolution in the spectrum frequency, or an inhibitor that is not functioning properly [39].

IE increases with increasing the concentration of the inhibitors as shown in Table 3. IE decreases with the increment of the temperature as it is shown in Table 4. This result suggests that the inhibitor molecules adsorb physically on the mild steel surface and not chemically; therefore, increasing temperature enhances both the dissolution of metal and the desorption of inhibitor molecules from the metal surface.

The corrosion parameters, including corrosion efficiency (IE%), corrosion current density (μA cm^{-2}), Tafel constant and causality
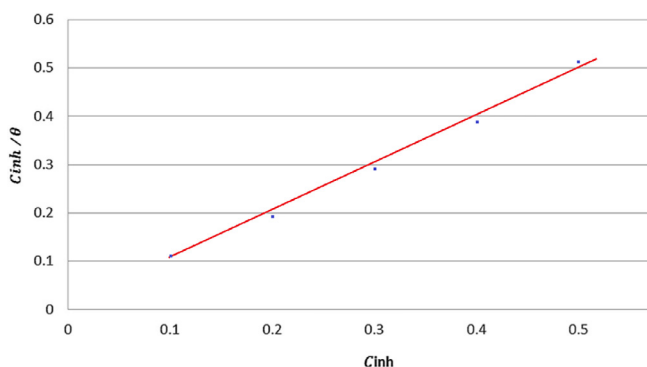
Table 3
Electrochemical frequency modulation (EFM) parameters for mild steel in 1.0 M HCl with various concentrations of the corrosion inhibitor at 30 °C.

Concentration (mM)	i_{corr} (mAcm^2)	β_1 (mVdec^{-1})	β_2 (mVdec^{-1})	Corrosion Rate (mpy)	IE_{EFM} (%)	CF-2	CF-3
0.00	0.1965	75.90	88.12	174.81	0.00	1.685	4.027
0.30	0.1271	101.94	114.27	97.45	35.32	1.407	2.77
0.40	0.0977	114.65	120.30	83.85	50.28	0.834	4.207
0.50	0.0648	119.11	131.62	62.75	67.02	0.678	3.448

Table 4
EFM parameters for mild steel in 1.0 M HCl with 0.5 mM of the corrosion inhibitor at various temperatures.

Temp. (°C)	Concentration (mM)	i_{corr} (mAcm^2)	β_1 (mVdec^{-1})	β_2 (mVdec^{-1})	Corrosion Rate (mpy)	IE_{EFM} (%)	CF-2	CF-3
30	Blank	0.1965	75.90	88.12	174.81	0.00	1.685	4.027
30	0.50	0.0648	119.11	131.62	62.75	67.02	0.678	3.448
40	Blank	0.2785	88.58	119.27	281.57	0.00	1.731	1.715
40	0.5	0.1716	109.79	123.96	165.34	38.38	1.782	3.833
50	Blank	0.3657	91.02	122.13	363.08	0.00	1.855	4.268
50	0.5	0.2953	119.17	131.78	162.94	19.25	1.752	3.493
60	Blank	0.268	96.99	132.07	183.97	26.72	391.5	4.791
60	0.5	0.4951	128.86	142.06	362.86	10.26	3.844	3.112

Fig. 5. Langmuir's isotherm adsorption synthesized corrosion inhibitor on the mild steel surface in 1.0 M HCl at 303 K.

factors (CF-2 and CF-3), are listed in Tables 3 and 4 for different concentrations of the corrosion inhibitor in 1.0 M HCl at 30 °C and at different temperatures, respectively.

Adsorption isotherm

Adsorption isotherms can provide basic information about the interaction between the inhibitor and mild steel surface [40]. The corrosion inhibition of organic inhibitors on mild steel in sulfuric acid can be explained via the molecular adsorption method. The adsorption process is influenced by the structure of the organic compounds, the charge distribution in the molecules, the nature of the surface-charged metals and the types of media used [41]. The phenomenon of interaction between the metal surface and the inhibitor can be better understood in terms of the adsorption isotherm. The plots of Cinh/θ as in Fig. 5, against Cinh yield a straight line with an approximately unit-slope, indicating that the inhibitor under study obeys the Langmuir adsorption isotherm [42], as in the equation below.

$$\text{Cinh}/\theta = (1/K_{ads}) + \text{Cinh} \tag{3}$$

where Cinh is the concentration of the inhibitor and K_{ads} is the adsorption constant obtained from the intercept of the straight line.

Generally, the corrosion inhibition mechanism in an acid medium is adsorption of the inhibitor on the metal surface. The process of adsorption is influenced by different factors like the nature and charge of the metal, the chemical structure of the organic inhibitor and the type of aggressive electrolyte [43].

Conclusions

In this manuscript, we presented for the first time a novel organic inhibitor which was tested and the changes in electrochemical impedance spectroscopy (EIS) and Electrochemical frequency modulation (EFM) measurements were utilized to study the corrosion inhibition of mild steel in 1.0 M HCl solutions at 30, 40, 50 and 60 °C, with the use of the inhibitor. This inhibitor exhibited a good inhibition performance as an organic inhibitor. This inhibitor has heteroatoms, O, and N that are found to have higher basicity and electron density and thus act as corrosion inhibitors. The acidic corrosion of mild steel was reduced by addition of appropriate novel inhibitor concentrations. The inhibition efficiencies increased with inhibitor concentration but were reduced proportionally with temperature. The inhibitor acts as an efficient corrosion inhibitor on a mild steel surface with a maximum inhibition efficiency of 59.36%.

Appendix A. Supplementary data

Supplementary data associated with this article can be found, in the online version, at https://doi.org/10.1016/j.rinp.2017.12.039.

References

[1] Shetty SD, Shetty P, Nayak HS. The inhibition action of N-(furfuryl)-N′-phenyl thiourea on the corrosion of mild steel in hydrochloric acid medium. Mater Lett 2007;61(11):2347–2349.
[2] Quraishi M, Shukla SK. Poly (aniline-formaldehyde): a new and effective corrosion inhibitor for mild steel in hydrochloric acid. Mater Chem Phys 2009;113(2):685–9.
[3] Musa AY, Jalgham RT, Mohamad AB. Molecular dynamic and quantum chemical calculations for phthalazine derivatives as corrosion inhibitors of mild steel in 1M HCl. Corros Sci 2012;56:176–83.
[4] Sastri VS. Corrosion inhibitors: principles and applications. New York: Wiley; 1998.
[5] Al-Amiery AA, Musa AY, Kadhum AAH, Mohamad A. The use of umbelliferone in the synthesis of new heterocyclic compounds. Molecules 2011;16:6833–43.
[6] Khan G et al. Application of natural product extracts as green corrosion inhibitors for metals and alloys in acid pickling processes-a review. Int J Electrochem Sci 2015;10(8):6120–34.
[7] Musa AY et al. A comparative study of the corrosion inhibition of mild steel in sulphuric acid by 4, 4-dimethyloxazolidine-2-thione. Corros Sci 2009;51(10):2393–9.

[8] Szklarska-Smialowska Z. Insight into the pitting corrosion behavior of aluminum alloys. Corros Sci 1992;33(8):1193–202.

[9] Tadros AB, Abd-El-Nabey B. Inhibition of the acid corrosion of steel by 4-amino-3-hydrazino-5-thio-1, 2, 4-triazoles. J Electroanalytical Chem Interfacial Electrochem 1988;246(2):433–9.

[10] Donnelly B et al. The effect of electronic delocalization in organic groups R in substituted thiocarbamoyl R CS NH 2 and related compounds on inhibition efficiency. Corros Sci 1978;18(2):109–16.

[11] Khaled K. Electrochemical investigation and modeling of corrosion inhibition of aluminum in molar nitric acid using some sulphur-containing amines. Corros Sci 2010;52(9):2905–16.

[12] Rani B, Basu BBJ. Green inhibitors for corrosion protection of metals and alloys: an overview. Int J Corros 2011;2012.

[13] Musa AY et al. Corrosion inhibitive property of 4-amino-5-phenyl-4H-1, 2, 4-triazole-3-thiol for mild steel corrosion in 1·0M hydrochloric acid. Corros Eng, Sci Technol 2010;45(2):163–8.

[14] Kiani M et al. Inhibitory effect of some amino acids on corrosion of Pb–Ca–Sn alloy in sulfuric acid solution. Corros Sci 2008;50(4):1035–45.

[15] Solmaz R et al. Investigation of adsorption and inhibitive effect of 2-mercaptothiazoline on corrosion of mild steel in hydrochloric acid media. Electrochim Acta 2008;53(20):5941–52.

[16] Bockris JM, Green M, Swinkels D. Adsorption of Naphthalene on Solid Metal Electrodes. J Electrochem Soc 1964;111(6):743–8.

[17] Al Amiery A, Kadhum A, Alobaidy A, Mohamad A, Hoon P. Novel corrosion inhibitor for mild steel in HCl. Materials 2014;7(2):662–672 24.

[18] Obayes H, Alwan G, Alobaidy A, Al-Amiery A, Kadhum A, Mohamad A. Quantum chemical assessment of benzimidazole derivatives as corrosion inhibitors. Chem Cent J 2014;8(21):27.

[19] Junaedi S, Kadhum AAH, Al-Amiery AA, Mohamad AB, Takriff MS. Synthesis and characterization of novel corrosion inhibitor derived from oleic acid: 2-Amino 5-Oleyl-1,3,4Thiadiazol (AOT). Int J Electrochem Sci 2012;7:3543–54.

[20] Al-Azawi K, Al-Baghdadi S, Mohamed A, Al-Amiery A, Abed T, Mohammed S, Kadhum A, Mohamad A. Synthesis, inhibition effects and quantum chemical studies of a novel coumarin derivative on the corrosion of mild steel in a hydrochloric acid solution. Chem Cent J 2016;10(23):1–9.

[21] Fayyad E et al. Evaluation techniques for the corrosion resistance of self-healing coatings. Int J Electrochem Sci 2014;9:4989–5011.

[22] Standard A. G1–03. Standard Practice for preparing, cleaning, and evaluating corrosion test specimens. Annual Book ASTM Standards 2003;3:17–25.

[23] Macdonald DD. Reflections on the history of electrochemical impedance spectroscopy. Electrochim Acta 2006;51(8):1376–88.

[24] Jüttner K. Electrochemical impedance spectroscopy (EIS) of corrosion processes on inhomogeneous surfaces. Electrochim Acta 1990;35(10):1501–8.

[25] Park J, Macdonald D. Impedance studies of the growth of porous magnetite films on carbon steel in high temperature aqueous systems. Corros Sci 1983;23(4):295–315.

[26] Walter G. A comparison of single frequency and wide frequency range impedance tests for painted metals. Corros Sci 1990;30(6):617–29.

[27] Walter G. The application of impedance methods to study the effects of water uptake and chloride ion concentration on the degradation of paint films—I. Attached films. Corros Sci 1991;32(10):1059–84.

[28] Mansfeld F. Electrochemical impedance spectroscopy (EIS) as a new tool for investigating methods of corrosion protection. Electrochim Acta 1990;35(10):1533–44.

[29] Al-Moubaraki AH, Al-Judaibi A, Asiri M. Corrosion of C-steel in the Red Sea: effect of immersion time and inhibitor concentration. Int J Electrochem Sci 2015;10:4252–78.

[30] Soltani N et al. Green approach to corrosion inhibition of 304 stainless steel in hydrochloric acid solution by the extract of Salvia officinalis leaves. Corros Sci 2012;62:122–35.

[31] de Souza FS, Spinelli A. Caffeic acid as a green corrosion inhibitor for mild steel. Corros Sci 2009;51(3):642–9.

[32] Musa AY et al. Corrosion inhibition of mild steel in 1.0 M HCL by amino compound: Electrochemical and DFT studies. Metall Mater Trans A 2012;43(9):3379–86.

[33] Khaled K, Al-Qahtani M. The inhibitive effect of some tetrazole derivatives towards Al corrosion in acid solution: Chemical, electrochemical and theoretical studies. Mater Chem Phys 2009;113(1):150–8.

[34] Al-Amiery AA et al. A novel hydrazinecarbothioamide as a potential corrosion inhibitor for mild steel in HCl. Materials 2013;6(4):1420–31.

[35] Singh AK, Singh AK, Ebenso EE. Inhibition effect of cefradine on corrosion of mild steel in HCl solution. Int J Electrochem Sci 2014;9:352–64.

[36] Abdel-Rehim S, Khaled K, Abd-Elshafi N. Electrochemical frequency modulation as a new technique for monitoring corrosion inhibition of iron in acid media by new thiourea derivative. Electrochim Acta 2006;51(16):3269–77.

[37] Hermas A, Morad M. A comparative study on the corrosion behaviour of 304 austenitic stainless steel in sulfamic and sulfuric acid solutions. Corros Sci 2008;50(9):2710–7.

[38] Yohai L, Vázquez M, Valcarce M. Phosphate ions as corrosion inhibitors for reinforcement steel in chloride-rich environments. Electrochim Acta 2013;102:88–96.

[39] Khamis A, Saleh MM, Awad MI. The counter ion influence of cationic surfactant and role of chloride ion synergism on corrosion inhibition of mild steel in acidic media. Int J Electrochem Sci 2012;7:10487–500.

[40] Vracar LM, Drazic DM. Adsorption and corrosion inhibitive properties of some organic molecules on iron electrode in sulfuric acid. Corros Sci 2002;44:1669–80.

[41] Zhao TP, Mu GN. The adsorption and corrosion inhibition of anion surfactants on aluminium surface in hydrochloric acid. Corros Sci 1999;41:1937–44.

[42] Rubaye A, Abdulwahid A, Al-Baghdadi S, Al-Amiery A, Kadhum A, Mohamad A. Cheery sticks plant extract as a green corrosion inhibitor complemented with LC-EIS/MS Spectroscopy. Int J Electrochem Sci 2015;10:8200–9.

[43] Al-Amiery AA, Al-Majedy YK, Kadhum AAH, Mohamad AB. New coumarin derivative as an eco-friendly inhibitor of corrosion of mild steel in acid medium molecules. Molecules 2015;20:366–83.